

Single Photon Counting with a focus On Biomedical Applications

Nick Bertone, Musadi Wabuyele & Team, Achilles Kapanidis & Team, Henri Dautet and Murray Davies

The new 4-channel SPCM array from Excelitas is introduced and the main application - “Single Molecule Detection” for the array is discussed in detail. An example of single molecule detection is presented - this example will examine new strategies for analyzing molecular signatures of disease states in real time using single pair fluorescence energy transfer (spFRET) to rapidly detect point mutations in unamplified genomic DNA.

Introduction:

Over the past few years a growing number of companies have come to rely on Photon Counting for applications that range from particle sizing, atmospheric studies and advanced forms of biomedical research. Photon counting technology using Avalanche Photodiodes are achieving 70% photon detection efficiencies with sub nanosecond timing jitters and low dark counts (typically < 250cps). Besides being extremely small and rugged, these photon counting devices based on avalanche photodiodes have rapid recovery from overload, wide dynamic range and very low afterpulsing probabilities.

In biomedical instruments, fluorescence detection can be accomplished with simple photodiodes, photomultiplier tubes (PMT's), Charged Couple Devices (CCD's) and now photon counting devices. The detection technology depends on the performance and type instrument to be developed. For example, a simple fluorescence system would use a flash lamp to excite the sample and a simple detector (Silicon PIN or PMT) to detect the fluorescence intensity. For high throughput screening instrumentation, lasers and scanning optics are used to excite the multi-array plate and CCD's to measure the intensity of all wells at once.

New technology based on Single Molecule Detection use confocal microscope and photon counting technology to excite and detect single photons fluorescing from these single molecules. Because of the small sample sizes, speed of counting and sensitivity of the overall system, this technology allows for collecting multiple parameters such as: Fluorescence intensity, molecule diffusion times, fluorescence lifetime measurements and fluorescence polarization information.

The SPCM, why it works:

There are two reasons for the success of the SPCM. First is the ability to detect from a few to several million photons per second, second its high single photon detection efficiency.

At the heart is the Slik™ Avalanche Photodiode (APD). APDs are semiconductor junctions operated under reversed bias. Under these conditions, they exhibit an electric field profile that will multiply, through impact ionisation, electrons generated inside the material (bulk generation). A sketch of the multiplication process is displayed Figure 1.

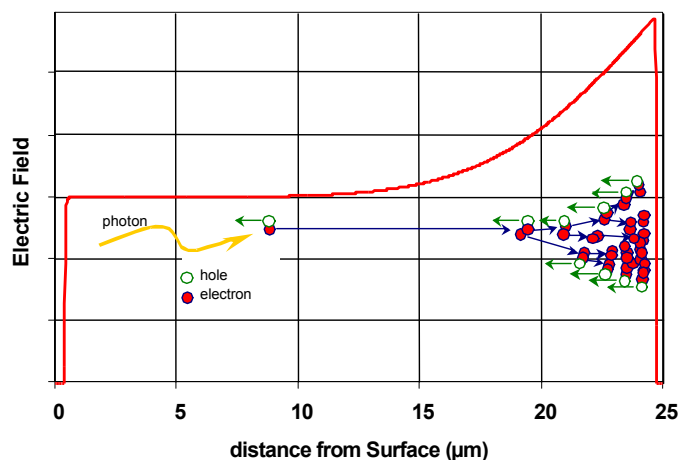


Figure 1 Electron multiplication process

Impact ionisation is a strong function of the electric field; as a result, the gain is a function of the detector bias, and a typical gain curve for the Slik™ is displayed Figure 2.

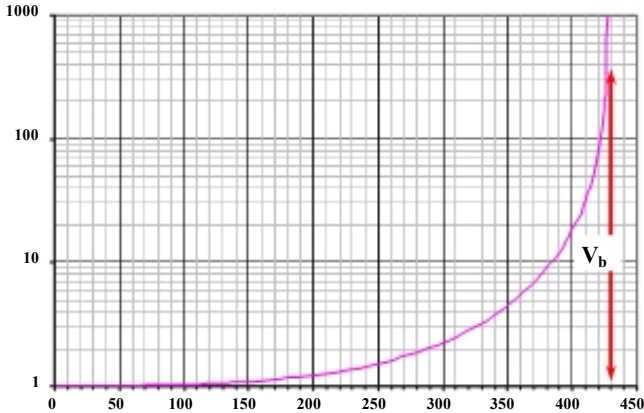


Figure 2 Typical gain curve of a Slik APD

It may be seen that at a certain bias, the gain tends asymptotically to infinity. This is the so-called breakdown voltage (V_b). Since the goal is to detect the single electron generated by a single photon, the only way to obtain a detectable signal is to generate as high a gain as possible, which implies operations under breakdown conditions.

Most semi-conductor junctions of even much smaller size than the Slik™ generate of the order of tens of millions of electrons per second (bulk leakage current of the order of pA). In this case operation above V_b , would, if not current limited, burnout the chip in a short time, or if current limited result in a steady current and the detector would be completely useless for photon detection.

The difference with the Slik™, results from its extremely low bulk leakage current. When cooled to -10°C as few as tens of thermally excited electrons per second are generated in the dark (this is the dark-count or DC). Such a low level of thermal electrons can only be achieved through extreme attention to the quality of both material and processing. Since there is such a large time laps between “dark” electrons, there is time to “quench” the avalanche and ready the detector for the next photoelectron. Quenching is performed by sensing the onset of the avalanche, the sensing circuit then sends a signal to both the quenching circuit that lowers the bias in a few nanoseconds below V_b , and the output circuit that sends a TTL signal to the output BNC after a suitable delay to ensure all charges have left the drift region, the reset circuit is activated and all components (including the detector) reset to their original value in order for the Slik™ to be ready for the next photoelectron. This “quenching and reset” process takes of the order of 50 ns and is called the “dead-time”.

The other important characteristic of the SPCM is the high single photon detection efficiency (P_d). There are two reasons for it. First the detector being in silicon exhibits the silicon characteristic that is high quantum efficiency from the UV to the near-infrared as shown in Figure 3.

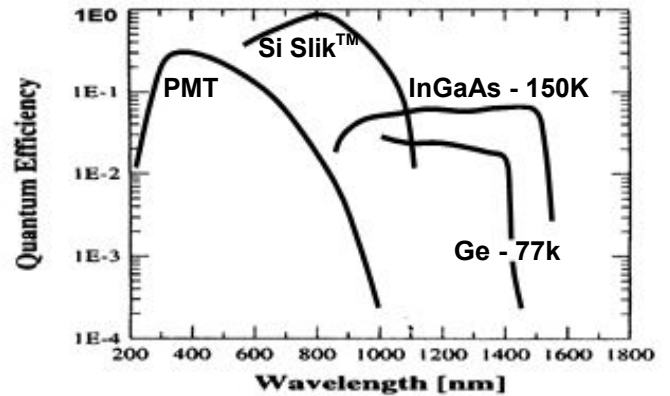


Figure 3 Typical QE curves of a various photo detectors..

Second by operating sufficiently high above the breakdown, one ensures that nearly all electrons induce a junction breakdown, thus resulting in a detectable pulse.

Slightly less important for some applications but critical for most is the real time output of the SPCM.

The 4-channel SPCM Array:

The single channel SPCM with its superior photon detection efficiencies in the 500nm to 1000nm range and its ease of use, has been making progress in being designed into biomedical instrumentation - especially in instruments based on **single molecule detection**. With the single channel SPCM multiple colors, polarizations and diffusions can be analyzed only one measurement at a time. If the user required all measurements to be done at the same time - one SPCM would be required per measurement to be performed. Therefore, if a user wanted to examine 4 colors per well and four wells at one time, 16 channels/SPCM's would be required. Figure 4 shows a system with 36 channels, this of course would not be feasible for most biomedical instrumentation. With the 4-channel SPCM shown in Figure 5, with its reduced cost and compact size a 36-channel system will now be economically feasible.

With the compact size of the SPCM, systems with 25 arrays or 100 channels can be envisioned, allowing for the collection of multiple parameters per pixel and

multiple pixels at a time. The information required for developing new drugs, analyzing genes, proteins and cells will require the ability to detect multi-parameters such as: fluorescence intensity, diffusions, lifetimes and polarizations in a timely and efficient manner. Single Molecule Detection Technology allows for quick and efficient collection and measurement of these parameters and the SPCM array is the detector of choice in this new and exciting technology.

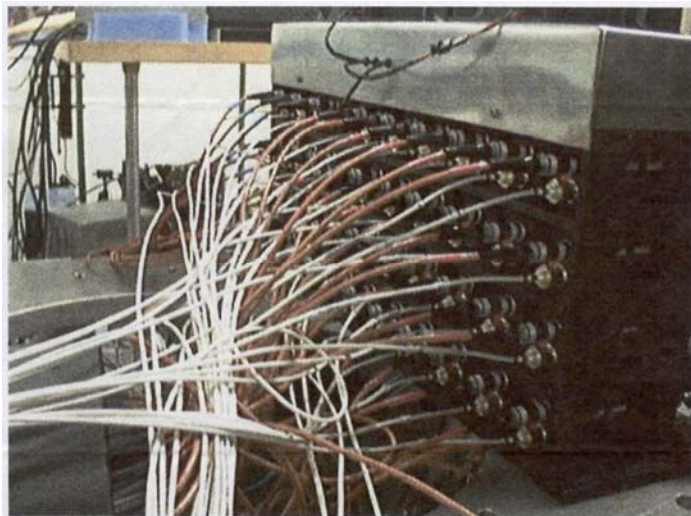


Figure 4 System with 36 channels



Figure 5 4-channel SPCM

Single-molecule detection (A. Kapanidis & the UCLA Team)

By single-molecule detection, we refer to the ability to observe and analyze individual molecules, one-molecule-at-a-time; such analysis contrasts

conventional methods which draw their signals from ensembles of millions of molecules. Combining confocal optics with point-detection, we observe single diffusing or surface-immobilized species.

For analyzing diffusing species, we use sub-nanomolar solutions of such species to ensure that the detection volume is occupied by --at most-- one molecule at a given time. As shown in Figure 4, fluorescent molecules diffuse across a tightly-focused laser spot (green oval); this spot coincides with the confocal detection volume. When the molecule is out of the laser spot, there is no signal; when the molecule enters the laser spot, the fluorophore is excited by the laser and within nanoseconds emits a fluorescence photon (shown as yellow arrows); this cycle of excitation and emission is repeated thousands of times during the transit of the molecule from the laser spot, resulting in numerous photons that are detected by the APDs, generating fluorescence bursts. Residence times of fluorescent species in the detection volume are typically 0.1-10 ms, depending on the size of the detection volume, the size of the diffusing species, and the viscosity of the solution.

For analyzing surface-immobilized species, similar principles apply, with the difference that the movement of the fluorescent molecules in and out of the detection volume is controlled by a piezo-electric stage. We immobilize fluorescent species on glass; focus the laser spot on the surface, and raster-scan the surface (usually a 5x5 to 40x40 μm area). When the molecule is out of the laser spot, there is no signal; when the stage brings a molecule in the laser spot, the fluorophore is excited by the laser and emits a fluorescence photon; this cycle of excitation and emission again results in fluorescence-bursts for every x-line of scanning. Then, the stage moves along the y-axis, and the x-scan is repeated. Finally, the x-lines are combined to reconstruct an image of the immobilized sample.

For single-molecule detection, we use a custom confocal fluorescence microscope that combines high numerical-aperture optics with ultra-sensitive detection as illustrated in Figure 5. Our excitation sources are red and green lasers that allow excitation of various fluorophores in the visible range. The laser lights go through electrooptical modulators that allow alternation of laser excitation if necessary. The laser beams are then coupled to fiber optics, reflected on a dichroic mirror, and focused by a high NA objective in a T-controlled flow cell that holds the sample. The sample is either in solution, a gel matrix or on a glass surface. Fluorescence emitted from the sample is collected through the objective and dichroic, spatially-filtered

through a pinhole, spectrally-filtered through a dichroic mirror and filters, and focused on the active area of APDs.

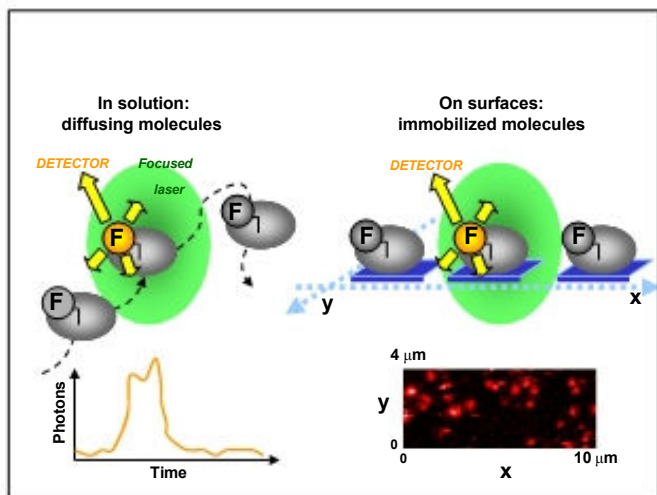


FIGURE 6 Single molecule detection using point detectors

The photon arrival time is recorded by an acquisition board, and the data are visualized and stored on a PC. Although only 2 APDs are shown here, our custom microscope is equipped with 4 APDs, that allow monitoring of up to 4 spectral regions, or of the 2 polarization components of 2 spectral regions, thus permitting experiments of unprecedented sophistication.

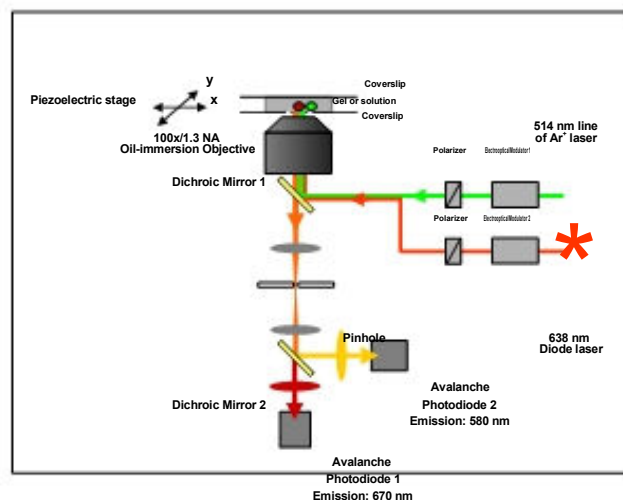


FIGURE 7 Single-molecule confocal microscopy

FÖRSTER RESONANCE ENERGY TRANSFER (FRET):

Using single-molecule detection to analyze fundamental biological questions, such as transcription of DNA, protein folding and protein aggregation, as well as to develop assays to monitor protein-DNA, protein-protein and protein-drug interactions. To monitor structures and interactions, Forster resonance energy transfer (FRET) is used. This method acts as a “molecular ruler” that allows measuring distances of 2-10 nm within molecules and complexes as shown in figure 6.

Assume we have a pair of fluorescent probes with significant spectral overlap, named D (for donor) and A (for acceptor). After exciting of D, a fraction of its energy is transferred to the A through a dipole-dipole interaction between the probes. The efficiency of this transfer (designated as E) is a sensitive function of the distance R between the two probes, as shown in the equation, and can be used to evaluate distances. When D-A are close, the efficiency is high, the D emission is low and the A emission is high. When D-A are far, the efficiency is low, the D emission is high and the A emission is low.

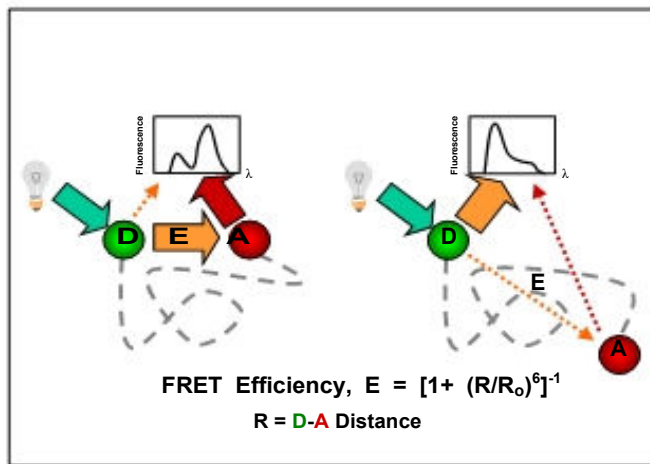


FIGURE 8 A “Molecular Ruler” for the 2-10 nm regime

Single protein DNA complexes can be observed and analyzed using single-molecule detection. Complexes are prepared in solution or through gel purification and observed as diffusing species, shown in Figure 7 as fluorescence bursts or as surface-immobilized species shown as fluorescence spots. Information obtained from both formats allows us:

- To identify subpopulations (by analyzing D-A intensity 2D-histograms; we can clearly see species 1 and 2 here)

- To monitor structure (by evaluating D-A distances in distinct species seen in *E*-histograms; for example this high FRET peak corresponds to a D-A distance of ~30Å) and
 - To monitor dynamics (by looking at D and A intensity changes during the available observation window, as seen for this diffusing species).

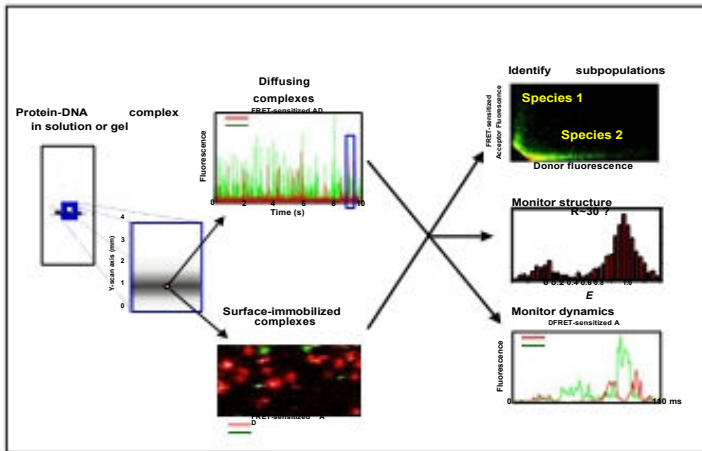


FIGURE 9 Analysis of single protein-DNA complexes

FRET ON IMMOBILIZED PROTEIN-DNA COMPLEXES

Protein-DNA complexes that show high FRET (D-A are close in space). A high-FRET complex will have low D emission and high A-emission. After surface-immobilization, we excite the sample with a green laser (that CANNOT excite A directly), and monitor D and A emission using 2 Excelitas SPCM's. High D emission (left panel in Figure 8) points to species that do not participate in FRET;

High A emission (middle panel) points to species that participate in high FRET. Overlay of the two emissions allows us to see the ratio of the no-FRET/high-FRET species (compare green and red spots). This can also be done more rigorously by calculating FRET for every pixel by that using the D-emission and A-emission intensity for every pixel; the FRET results are summarized in histograms. Such analysis reveals:

- 1, The presence of an interaction (no interaction will show no FRET; A-emission image will have no spots)
- 2, the specificity of the interaction (non-specific interactions do not result in high-FRET, so the histogram will look extremely different)
- 3, the existence of subpopulations or free species (as seen in the histogram showing two peaks)

4-structural features of the complex, since we can measure the exact distance between D-A (here ~30 Angstrom)

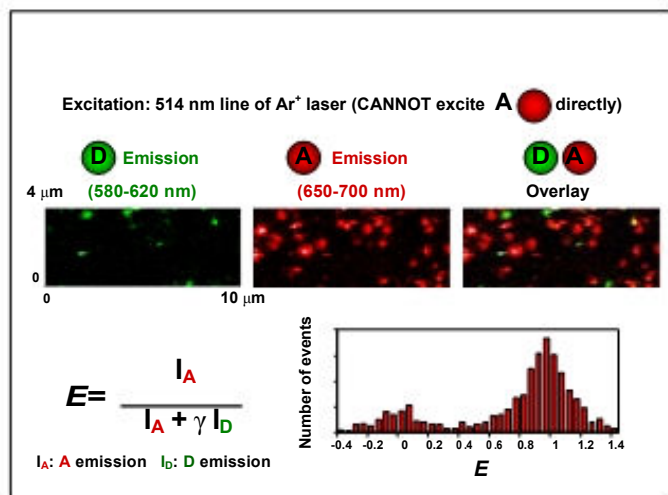


FIGURE 10 FRET on immobilized protein-DNA complexes

We can also focus on a single high-FRET complex and obtain ms-timescale time-trajectories of the D and A emission signals, figure 9 - left panel. This allows us:

- 1, to obtain dynamic information about the system (for example, transient changes of D-A distance). This can be done with the first portion of the trace, where both D and A are present.

- 2-We can also determine the stoichiometry of an interaction by looking at the various signal levels during the time trace. In this trace, a single A-emission signal is seen, pointing to one A-fluorophore in the complex. Upon bleaching of the acceptor, A-emission decreases, and D-emission increases. The D also bleaches in a single-step. These observations assign an 1:1 stoichiometry to this complex. This can be also seen for an image, if we increase the laser intensity (right panel). Raster scanning (left to right, then top to bottom) allows observation of FRET-induced A-emission (red part of a spot), then the A bleaches and the D emission comes up (green part of a spot), and then D bleaches (spot disappears).

This technology will allow determination of enzymatic activity on surfaces and will allow reactions pathways to be observed from beginning to end.

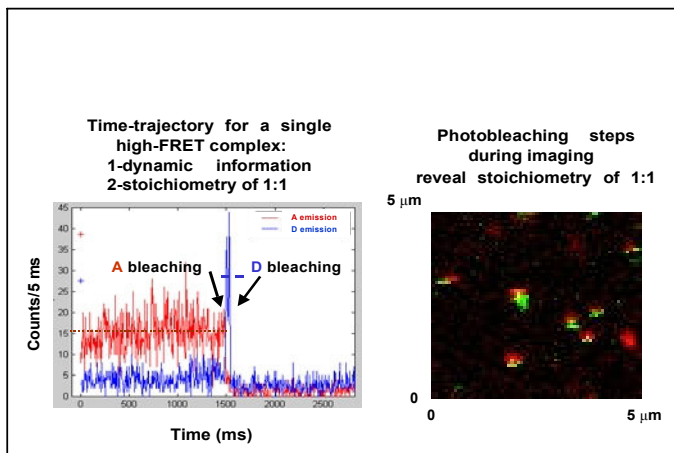


FIGURE 11 FRET on immobilized protein-DNA complexes (cont.)

FRET ANALYSIS USING ALTERNATE LASER EXCITATION (ALEX)

There are however, a few limitations for use of FRET to study interactions, some arising from complex photophysics of fluorophores, and some from the requirement of D-A proximity for FRET.

To overcome such limitations, we developed an excitation scheme that alternates rapidly between the green laser (that probes the donor in a direct fashion, and the acceptor in an indirect, FRET-dependent fashion) and a red laser (that probes the acceptor in a direct, FRET-independent fashion). Different species in our biochemical system, for example for a $A+B \leftrightarrow AB$ interaction, will yield distinct emission “signatures”, allowing easy differentiation of various species in our reactions and allow determination of binding constants. Figure 10 shows:

The A-only species (that corresponds to free AA) will show A emission when excited by the red laser

The D-only species (that corresponds to free BB) will show D emission when excited by the green laser

The D-A species with high-FRET (that corresponds to AAB where D and A are close) will show A emission

when excited by the red laser, and mainly A emission when excited by the green laser (due to high FRET)

The D-A species with low-FRET (that corresponds to AAB where D and A at ANY distance) will show A emission when excited by the red laser, and mainly D emission when excited by the green laser (due to low FRET).

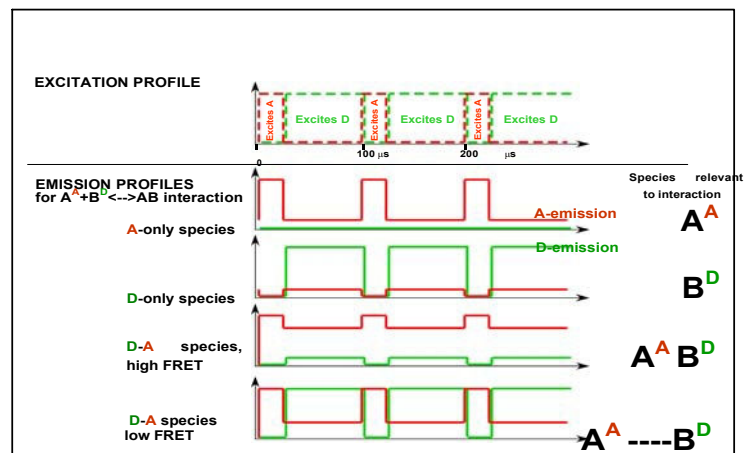


FIGURE 12 FRET analysis using alternate laser excitation (Alex)

To translate the different signatures into quantities that allow sorting, we use two ratios for every fluorescent species shown in Figure 11:

1-the familiar FRET ratio, and

2-a new ratio we call Alternate-laser-excitation emission ratio or ALEX. ALEX is the ratio of the green-laser-dependent emissions over the sum of green-laser-and red-laser dependent emissions.

Importantly, ALEX ratio can easily differentiate between the species involved in the interaction; D-only species result in high ALEX values, D-A species (with ANY D-A distance) result in intermediate ALEX values, A-only species result in low ALEX values

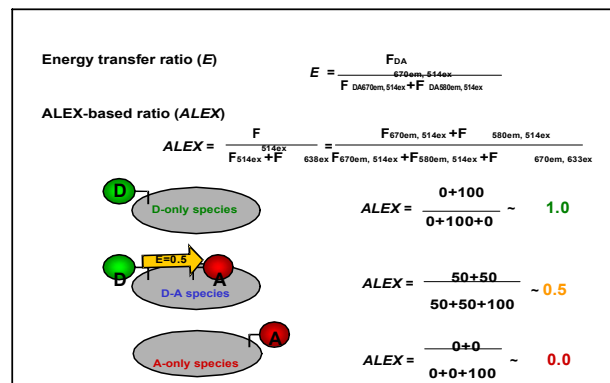


FIGURE 13 ALEX equations

As shown on Figure 13, using the E and ALEX ratios for each species, we can prepare two dimensional histograms of ALEX and E that sort the various species.

The ALEX axis sorts the various species in terms of stoichiometry; collapse of the data on the ALEX axis

allow binding information to be obtained. The E axis sorts the various D-A species in terms of D-A distance, collapse of the data on the E axis allow structural information to be obtained. Ratio of A-only/D-A species or D-only/D-A species can generate binding curves that characterize interactions, making this method powerful for analysis of protein-DNA, protein-protein and other interactions.

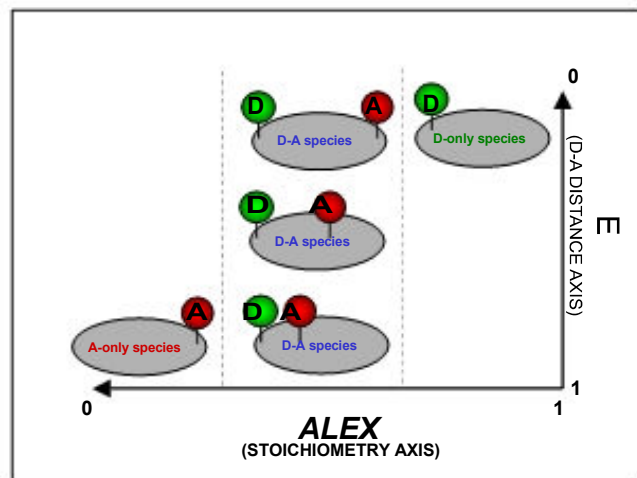


FIGURE 14 Sorting species using *E. Alex*

UCLA explored the capabilities of the ALEX-based method using fluorescently-labeled double-stranded DNA fragments carrying D and A probes separated by ~4, 7, and 11 nm, corresponding respectively to high, low and zero-FRET species

For the “high-FRET” DNA, figure 13 shows the clear separation of D-A species from D-only and A-only species. The D-A show high FRET and intermediate ALEX, as expected. This is also reflected in the individual ALEX and E histograms. Moving the A further away from the D (as in low-FRET DNA), does not change the ALEX ratio of D-A species, but lowers the E between them, as expected. Moving the A even further away from the D (as in zero-FRET DNA), once more does not change the ALEX ratio of D-A species, but lowers the E between them even further, as expected.

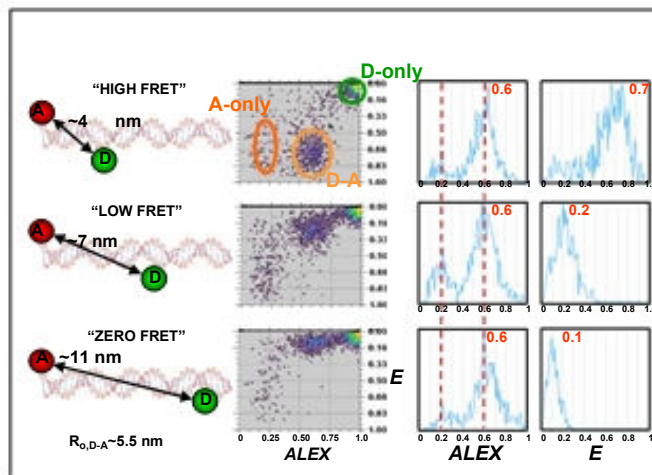


FIGURE 15 Model systems: *dsDNA*

Approaching real time molecular diagnostics: Single-pair fluorescence resonance energy transfer (spFRET) detection for the analysis of low abundant point mutations in K-ras oncogenes

(Musundi B.Wabuye & The Louisiana State University Team)

Diseases such as cystic fibrosis, Alzheimer’s, sickle cell anemia and certain cancers are associated with changes in the sequence of particular gene fragments. These changes can serve as biomarkers and may be useful for medical diagnosis at early stages of the disease. Since the majority of mutations in genetic disorders are due to variations such as point mutations, insertions or deletions, it is required that diagnostic techniques being developed have the capability of distinguishing these changes in a mixed population, where in most cases the mutant allele is the minority. In addition, DNA diagnostic methods should be rapid, highly sensitive, cost-effective, and easy to perform.

Current approaches used to detect single nucleotide variations (point mutations) include, homogenous methods such as the template directed dye terminator incorporation (TDI) assay,ⁱ the 5'-nuclease allele specific hybridization TaqMan assay,^{ii,iii} the allele specific molecular beacon assay^{iv,v} and ligase detection reaction (LDR).^{vi,vii,viii} These assays utilize fluorescence resonance energy transfer (FRET) to distinguish normal from mutant DNA without requiring a separation step, typically incorporated in most

heterogeneous assays. In general, these FRET-based methods require pre-amplification of genomic DNA via PCR. As illustrated in Scheme 1, diagnostic assays involve extraction of genomic DNA from either tissue, blood or stool samples followed by PCR amplification of the gene fragment carrying the mutation. However, PCR has limitations that make it difficult to quantitatively analyze and detect small genetic variations due to nonlinearities in amplicon number with cycle number and reduced specificity. In addition, long optimization and set up times, long run and analyses times and the high level of inherent inaccuracy and variation (due to cross-contamination) and the narrow dynamic range limits mutation screening assays incorporating PCR to perform quantitative measurements in real time.

Single molecule photon burst detection offers a unique opportunity to monitor the presence of unique sequences directly in genomic DNA without a PCR amplification step (see Scheme 1). In one such report, Castro and coworkers developed a method for the rapid, direct detection of specific nucleic acid sequences in biological samples.^{ix} In another report, specific DNA sequences in a homogeneous assay were detected using labeled hairpin-shaped oligonucleotide probes (Smart-Probes) in combination with single molecule detection.^x In this paper, we wish to report on a rapid, potentially real-time mutation detection scheme capable of detecting low abundant point mutations directly from unamplified genomic DNA samples. The detection scheme is illustrated in Figure 1. A ligase-based point mutation detection assay that uses an allele-specific discriminating primer and a common primer, each having a 10 base pair (bp) complementary arm with fluorescent labels at their 5'- and 3'-ends, respectively, is used. A perfect match between the base at the 3'-end of the discriminating primer and the target allows DNA ligase to covalently join the two adjacent primers flanking the mutation site. The LDR product then undergoes a conformational change to form a hairpin structure. A reverse molecular beacon is formed by the complementary arm sequences of the ligated primers. The two probes attached at the end of the arms are brought into close proximity by the hybridization and thus, energy transfer between the pair of probes occurs. Fluorescence emission resulting from the single-pair FRET process can be detected in real-time using single molecule detection.

Real-time spFRET measurements were performed in a poly(methylmethacrylate) (PMMA) microfluidic device to detect reverse molecular beacons (perfectly matched LDR products) formed in an LDR assay where point mutations in K-ras codon 12 (highly

associated with colorectal cancer) were detected in unamplified genomic DNA samples. Also, we demonstrate the assay's capability to rapidly detect single point mutations in genomic samples at a sensitivity of 1:1000 without PCR amplification. Analysis times < 5 min were achieved using real time LDR-spFRET detection in the microfluidic device.

EXPERIMENTAL SECTION

Microfluidic devices. spFRET was performed in a microfluidic device fabricated using a photolithographic procedure described elsewhere.^{xi} Briefly, microstructures were fabricated using LIGA (German acronym for lithography, electroplating and molding) processing. A thin layer of PMMA was glued onto a stainless steel metal plate and exposed to X-rays through an X-ray mask to form the desired patterns. The exposed PMMA resist was removed using GG After mechanically milling of the microstructures to the appropriate height, nickel was electroplated into the PMMA voids on the stainless steel from a Ni-sulfamate bath, then planarized and polished.

The mold inset fabricated as described above was mounted along with a PMMA substrate in an embossing machine. The mold insert and the substrate were heated above PMMA's glass transition temperature, T_g (107 °C), and pressed together using a controlled force (several kilonewtons) for 5 s and gradually cooled to a temperature below its T_g . The mold insert and substrate were then demolded, leaving the desired features in the PMMA polymer. A thin film of PMMA was used as a coverplate for the fabricated channel. This was carried out by clamping a molded PMMA substrate and the coverplate between two glass plates and thermally heating for 12 min at 107 °C and cooling to room temperature in a GC oven. Microdevices were fabricated in a "T" configuration and had channel sizes of 50 μm wide and 100 μm deep (see Figure 2).

Instrumentation. Single-pair FRET measurements were accomplished using a confocal fluorescence system shown in Figure 2. The excitation source consisted of a diode laser (635 nm, 56DIB142/P1, Melles Griot, Boulder, CO). The laser was directed onto a focusing objective using a dichroic mirror (690DRLP, Omega Optical, Brattleboro, VT). The objective was a 60X, 0.85 NA, microscope objective that was used to focus the laser to a 5 μm spot ($1/e^2$) into the microchannel resulting in a detection volume of ~1.5 pL. The fluorescence was collected by this same objective and transmitted through a set of filters specific for Cy5.5. The dichroic mirror transmitted the

emitted light from the acceptor and was filtered through another set of filters having a 690 nm longpass and bandpass filter (710DF10, Omega Optical, Inc, Brattleboro, VT). The light was then passed through a 100 μm diameter pinhole and focused onto the active area of a single photon avalanche diode (SPAD)

detector (SPCM-AQ-141, EG&G, Vandrioul, Canada) using a 20X objective. Transistor-transistor logic (TTL)

R pulses from the photodiode were counted by a PC-plug in board (PC100D, Advanced Research Instruments, Boulder, CO), stored and subsequently analyzed by a Pentium PC computer.

In most SMD applications, a molecular detection threshold discriminates individual fluorescence burst from fluctuations in the background photodistributions. The optimal molecular detection threshold value, therefore, maximizes the ability to distinguish between the actual molecular signature and the false positives at low analyte concentrations. This value is determined by evaluating both photocounts and molecular detection rate for blanks, controls and low concentration samples. In these experiments, molecular detection threshold values were chosen such that the average false positive rate was 0 s^{-1} . Histograms of fluorescence burst distributions for the single reverse MBs were accumulated using output values from the WQS filtered data set.

Results and Discussion

The design of our reverse-MB was also based on earlier studies where thermodynamic behaviors of partially self-complementary DNA molecules were studied.^{xii,xiii,xiv} According to these studies, it was observed that in aqueous solution at low concentrations, oligonucleotide molecules having a probe sequence flanked by two complementary arms may exist in equilibrium between two structured conformations: the dimeric duplex or monomeric hairpin. On increasing the temperature, the equilibrium shifted toward the hairpin conformation as shown in Figure 3. In addition, the authors showed that the melting of hairpins is a monomolecular process, since it is independent of the concentration, while duplex melting are bimolecular processes that are concentration dependent. Generally, single molecule detection requires the probability of single molecule occupancy within the detection volume be significantly smaller than unity to lower the probability of double occupancy. This can be achieved by diluting the samples to low concentrations and as such, the stability of the hairpin conformation over the duplex would be favored.

FRET depends on the inverse sixth power of the distance between the two probes (R^{-6}), with the efficiency (E) of energy transfer expressed as;

$$E = \frac{R_0^6}{(R_0 + r)^6} = 1 - \frac{F_{da}}{F_d} \quad (3)$$

where F_{da} is the fluorescence intensity of donor in the presence of acceptor, F_d is the intensity in the absence of acceptor, r is the distance between the donor and the acceptor. R_0 is known as Förster radius and is the distance at which 50 % of the donor's energy is transferred. Due to the large spectral overlap (~86 %) between Cy5 and Cy5.5 producing an exceptionally high R_0 value (63.3Å), flexibility in the choice of linker structures attaching the dyes to the MB could be used.

LDR primers were designed to detect point mutations in codon 12 of the K-ras gene associated with colorectal cancer.^{xv,xvi} For this particular mutation, the second position in codon 12, GGT, coding for glycine, mutates to GAT coding for aspartate, which can be detected by ligation of an allele-specific primer having a discriminating base (A) and a phosphorylated common primer. Using LDR primers designed specifically for the K-ras G12.2D mutation, LDR reactions were performed and the product was verified using capillary electrophoresis coupled to near-infrared laser-induced fluorescence.

Single-pair FRET detection. Typically, LDR assays are coupled to a primary PCR reaction with the amplicons used as the templates for the ligation reaction.^{xvii,xviii,xix} To evaluate the specificity of LDR directly on genomic DNA, we carried out spFRET studies using PCR products and genomic DNA extract from cell lines containing known K-ras genotype (HT29; wildtype and LS180; G12.2D mutation). Figure 3 show plots of the number of events detected at various threshold levels for an LDR assay having ~3,000 copies (10 ng) of initial wildtype and mutant template for both PCR product and genomic samples. A blank having no template was also analyzed. Applying 20 LDR cycles and assuming 100 % ligation efficiency for each cycle, one would expect ~60,000 LDR products. LDR samples were diluted by equal amounts of water to a concentration where the probability of occupancy (P_0) of a single hairpin was ~ 2.2×10^{-3} , which was calculated from,^{xx}

$$P_o = CN_A vP \quad (4)$$

where C is the concentration analyte, N_A is the Avogadro's number and P_v is the probe volume of 1.5 pL. The number of molecules passing through the probe volume per acquisition time (N_{ev}) was calculated from;^{xxi}

$$N_{ev} = \frac{2P v_{o ep}}{\pi \omega_o} \quad (5)$$

where v_{ep} is the migration velocity of DNA and ω_o is the $1/e^2$ beam waist (5 μ m). Therefore, with a concentration of ~30,000 copies in the 20 μ l sample well, we would expect ~28 events per 100 s. From Figure 6, we did not detect any events above threshold for either the wildtype PCR products or genomic DNA during the 100 s acquisition time. Conversely, we did observe events from LDR products formed by mutant samples having a T/A match. Six and 12 events were found above a threshold level from PCR product and genomic DNA samples, respectively. On applying this value a detection efficiency of 42 % was realized. These results indicated that LDR can be performed efficiently on genomic DNA directly.

Studies were next performed on genomic samples containing a minority of mutant templates in a majority of wildtype to determine the ability of detecting low abundant point mutations using spFRET. Figure 4A shows fluorescence bursts from LDR samples having 600 copies (2 ng) of mutant (12.2D) template in all reactions and changing the wildtype concentration with the ratio of mutant to wildtype varied from 1:1 to 1:1000. Clearly, histogram in Figure 4B show that single molecule events were observed above the threshold from samples having the point mutation even when 1000 normal templates to 1 mutant were evaluated. The ligation efficiency of our LDR assay having a vast majority mutant template was investigated. For accurate quantification of the low abundant mutant sequence in an excess of the wildtype sequence, we used a constant concentration of the mutant template (2 ng). The wildtype concentration was varied from 2ng to 2 μ g, resulting in a matched to mismatched ratio of 1:1 to 1:1000. From this result, we note that the addition mismatched template results in reduction in the formation of LDR hairpins, suggesting that the wildtype template acts as a competitive inhibitor in the assay. This phenomenon was also observed by Barany and co-workers.¹⁶

In our previous examples using spFRET, we eliminated the sample processing overhead associated with PCR and performed the allele-specific LDR directly on genomic DNA, even for low frequency mutant sequences. However, the assay still used linear amplification during LDR and a processing time for this step was 100 min (20 cycles). Therefore, we attempted to perform spFRET using only a single LDR thermal cycle to significantly reduce the processing time without sacrificing information content from spFRET. Figure 6 shows fluorescence photon bursts and histogram resulting from single LDR products linearly amplified using 1 mutant to 10 wildtype sequences. Over a 300 s data acquisition time, 5 ± 3.6 events from this sample was detected using only one cycle for LDR. The histogram indicated no product formed for 0 cycles. Similarly, the control sample having only the wildtype showed no bursts above threshold. A plot the number of events verses cycle number is shown in Figure 7. The plot was linear over a large dynamic range with a linear correlation coefficient of 0.989. The linear plot is consistent with the linear amplification process associated with LDR. Our data illustrates that spFRET coupled to LDR has the specificity to detect mutant sequences at a frequency of 0.1 directly from genomic DNA using a processing time < 5 min.

Conclusions

The exquisite sensitivity of single molecule detection can be used to eliminate processing steps required in multi-step assays, reducing analysis time. In the present example, we eliminated the need for PCR amplification and performed an allele-specific ligation assay directly on genomic DNA. In addition, the high sensitivity afforded by single molecule measurements also eliminated the need for thermal cycling during the ligation step. The specificity of the ligase enzyme toward mismatches coupled to spFRET of rMBs formed as a result of a successful ligation reaction for mutated DNA even in the presence of wildtype sequences provided real-time molecular diagnostic screening even when the copy number of target sequences was low (600 copies).

Many exciting applications can be envisioned for assays which employ real-time molecular diagnostic formats. For example, real-time detection of molecular signatures of specific tissue types could provide the surgeon information on what tissues to remove and what not to remove, which would be invaluable information for cancer procedures in delicate areas, such as the head or neck. In addition, the disease

state of tissues could be assessed directly in the surgical room during an endoscopic examination without the need for sending a biopsy sample to the pathologist, eliminating the need for an additional surgical procedure. Finally, screening of postal mail at high speeds for certain biological agents, such as anthrax, could be envisioned using simple assay protocols as that described herein. The ability to provide real-time sequence information would allow isolating potentially infected materials quickly and efficiently.

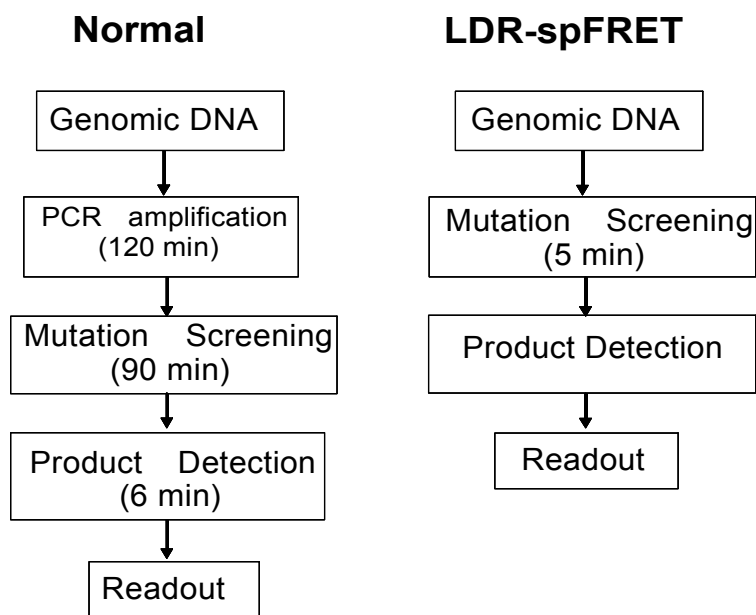
Future work -Time resolved detection of single LDR hairpins

Obtaining photophysical and spectral information on single molecule allow the utility of SMD in case where the analyte of interest is embedded in heterogeneous environment. In such case information that can not be revealed in ensemble measurement can now be obtained. One important physical property that can be monitored is the fluorescence lifetimes of the molecules. These property can be used to provides information on the sub-population in a heterogeneous mixture and also identify single molecules in a multiplex assays, where multiple probes labeled to unique target sequences are detected and analyzed. Figure 8, shows a schematic of the multiparameter confocal detection system equipped with SPAD detector that is currently being constructed for multiplexing..

References

1. Chen, X.; Kwok, Y. P. *Nucleic Acids Res.* **1997**, *25*, 347-353.
2. Holland, P.M.; Abramson, D.R.; Watson, R.; Gelfand, H. D. *Proc. Natl. Acad. Sci.* **1991**, *88*, 7276-7280.
3. Livak, K.J.; Marmaro, J.; Todd, A.J. *Nature Genet.* **1995b**, *9*, 341-342.
4. Tyagi, S.; Bratu, D.P.; Kramer, F.R. *Nat. Biotechnol.* **1998**, *16*, 49-53.
5. Tyagi, S.; Kramer, F.R. *Nat. Biotechnol.* **1996**, *14*, 303-308.
6. Barany, F.; *Proc. Natl. Acad. Sci.* **1991**, *88*, 189-193.
7. Chen, X.; Livak, K. J.; Kwok, Y. P. *Genome Res.* **1998**, *8*, 549-556.
8. Landgren, U.; Kaiser, R.; Sanders, J.; Hood, L. *Science*, **1988**, *241*, 1077-1080.
9. Castro, A.; Williams, J. G. K. *Anal. Chem.* **1997**, *69*, 3915-3920.
10. Knemeyer, J.; Marmé, N.; Sauer, M. *Anal. Chem.* **2000**, *72*, 3717-3724
11. Ford, S.M.; Davis, J.; Kar, S.; Qi, S.D.; McWhorter, S.; Soper, S. A.; Malek, C. K. *J. Biochem. Eng.* **1999**, *121*, 13-21.
12. Xodo, L.E.; Manzini, G.; Quadrifoglio, F.; van der Marel, G.A; van Boom, J. H. *Nucleic Acids Res.* **1986**, *14*, 5389-5398
13. SantaLucia, J. *Proc.Natl. Acad. Sci.* **1998**, *95*, 1460-1465.
14. Senior, M. M.; Jones, R.A.; Breslauer, K J. *Proc. Natl. Acad. Sci.* **1988**, *85*, 6242-6246.
15. Zhu, D.; Keohavong, P.; Finkelstein, S.D.; Swalsky, P.; Bakker, A.; Weissfeld, J.; Srivastava, S.; Whitesides, T.L. *Cancer Res.* **1997**, *57*, 2485-2492.
16. Bos, J.L. *Mutat. Res.* **1988**, *195*, 255-271.
17. Neiderhauser, C.; Kaempf, L.; Heinzer, I. *Eur. J. Clin. Microbiol. Infect. Dis.* **2000**, *19*, 477-480.
18. Khanna, M.; Cao, W.; Zirvi, M.; Paty, P.; Barany, F. *Clin. Biochem.* **1999**, *32*, 287-290
19. Khanna, M.; Park, P.; Zirvi, M.; Cao, W.; Picon, A.; Day, J.; Paty, P.; Barany, F. *Oncogene*, **1999**, *18*, 27-38.
20. Soper, S.A.; Legendre, B.L, *Appl. Spectrosc.* **1998**, *52*: 1-5.
21. Soper, S. A.; Mattingly, Q.; Vegunta, P. *Anal. Chem.* **1993**, *65*, 740-748.

Assay Overview



Scheme 1. An overview illustrating various analysis steps used in a diagnostic assay. The normal assay illustrates a typical PCR/LDR assay applying gel electrophoresis. The ligase detection reaction-single pair fluorescence resonance energy transfer (LDR-spFRET) is a real time screening/detection assay performed in microfluidic devices.

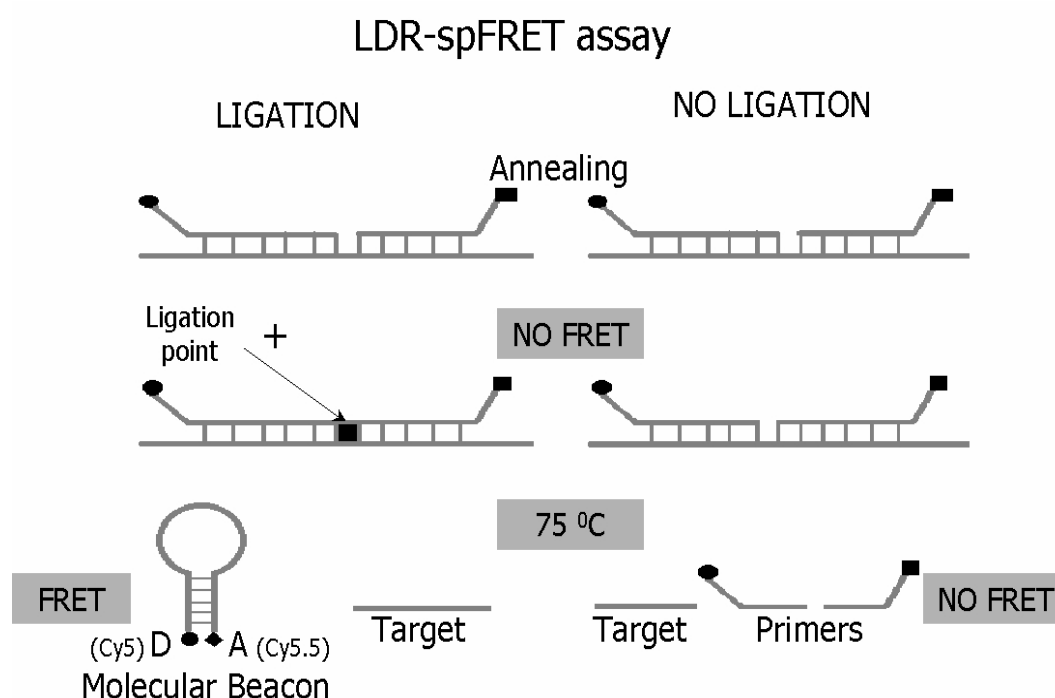


Figure 1. Illustrates an LDR-SpFRET assay in which two allele-specific primers that are labeled at the 3' and 5' ends with fluorescent probes, flank a mutation point on the template. Each primers has an extend arm sequence that is complementary to each other. Thermal stable DNA ligase enzyme covalently joined the two adjacent primers that are perfectly matched to the template, forming a hairpin (molecular beacon) that undergoes FRET. Conversely, the unligated primers do not show FRET. The detection temperature of the assay was maintained at 75 °C.

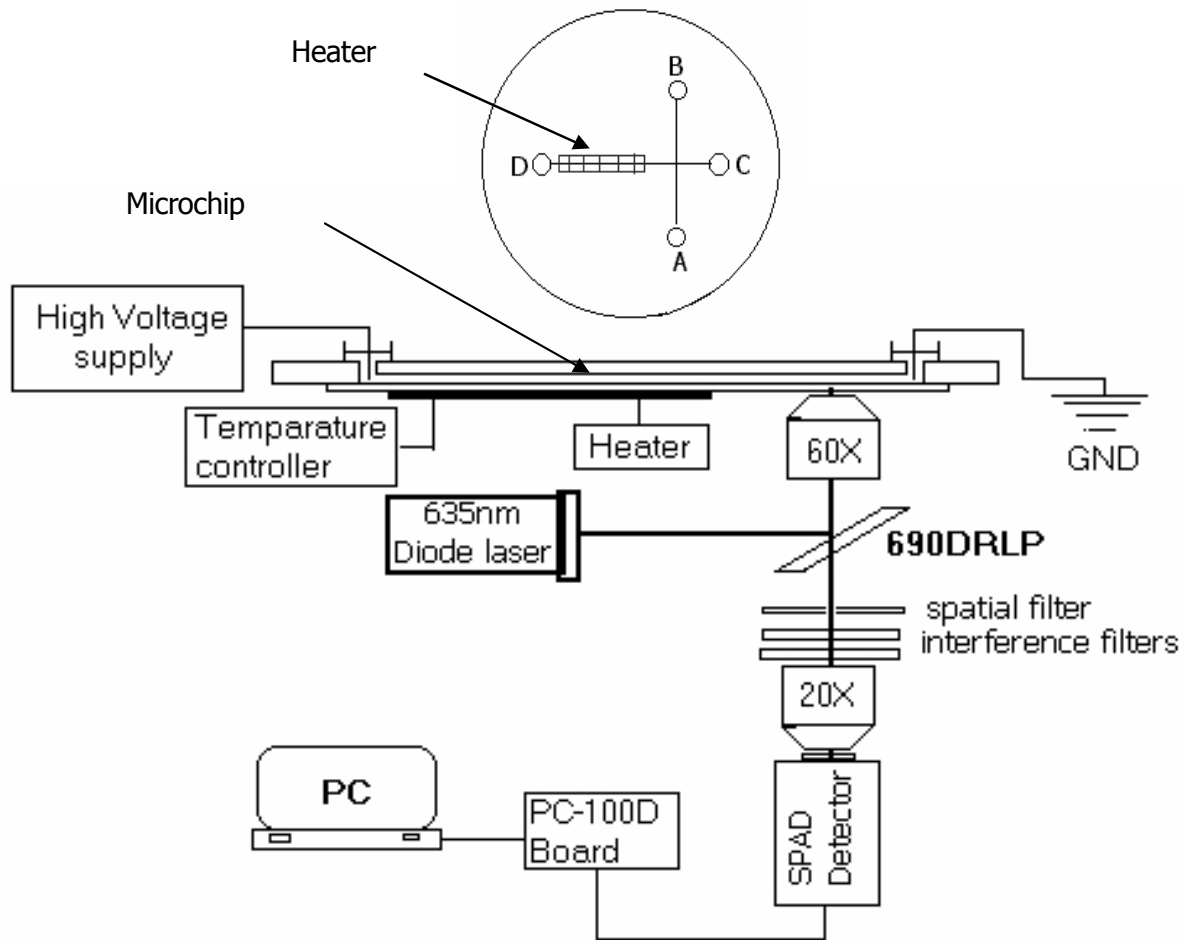


Figure 2. The confocal fluorescence detection system unit consisted of a diode laser ($\lambda = 635 \text{ nm}$) that was directed into a microscope objective using a dichroic and focused into the center of the fluidic channel approximately $\sim 1.5 \text{ cm}$ from the cross. Fluorescence was collected by this same objective and imaged onto a pinhole, through a set of FRET filters and finally processed using a single photon avalanche diode. A heater was attached at the bottom of the cover slip to regulate the assay temperature during detection

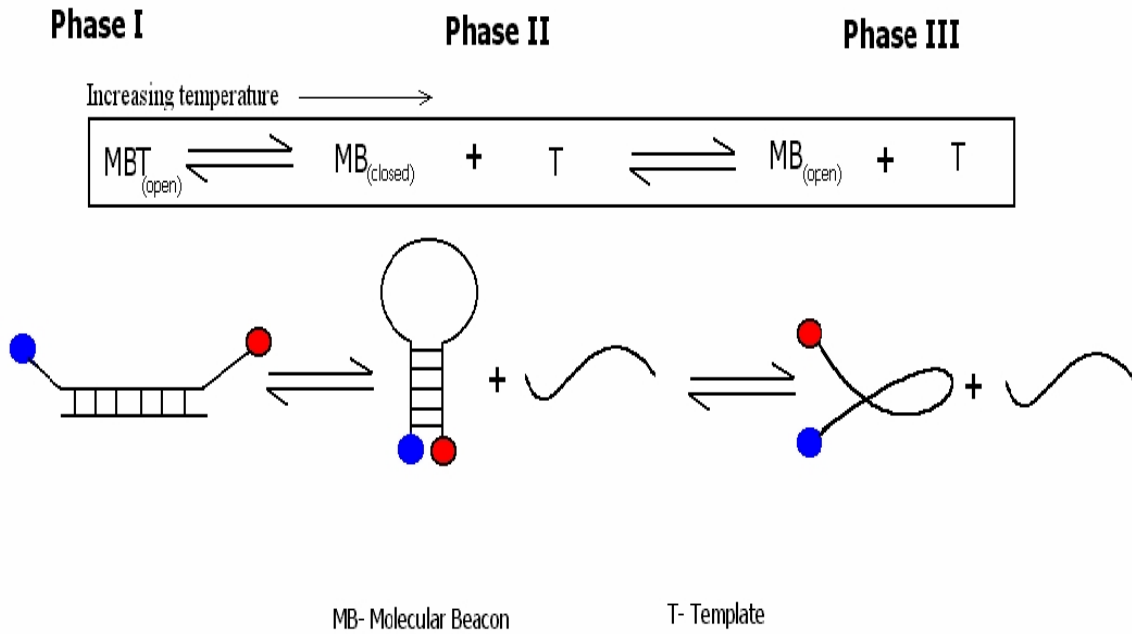


Figure 3. Structural phase transitions in solution of a molecular beacon having two fluorescent probes, donor and acceptor in the presence of a complementary template.

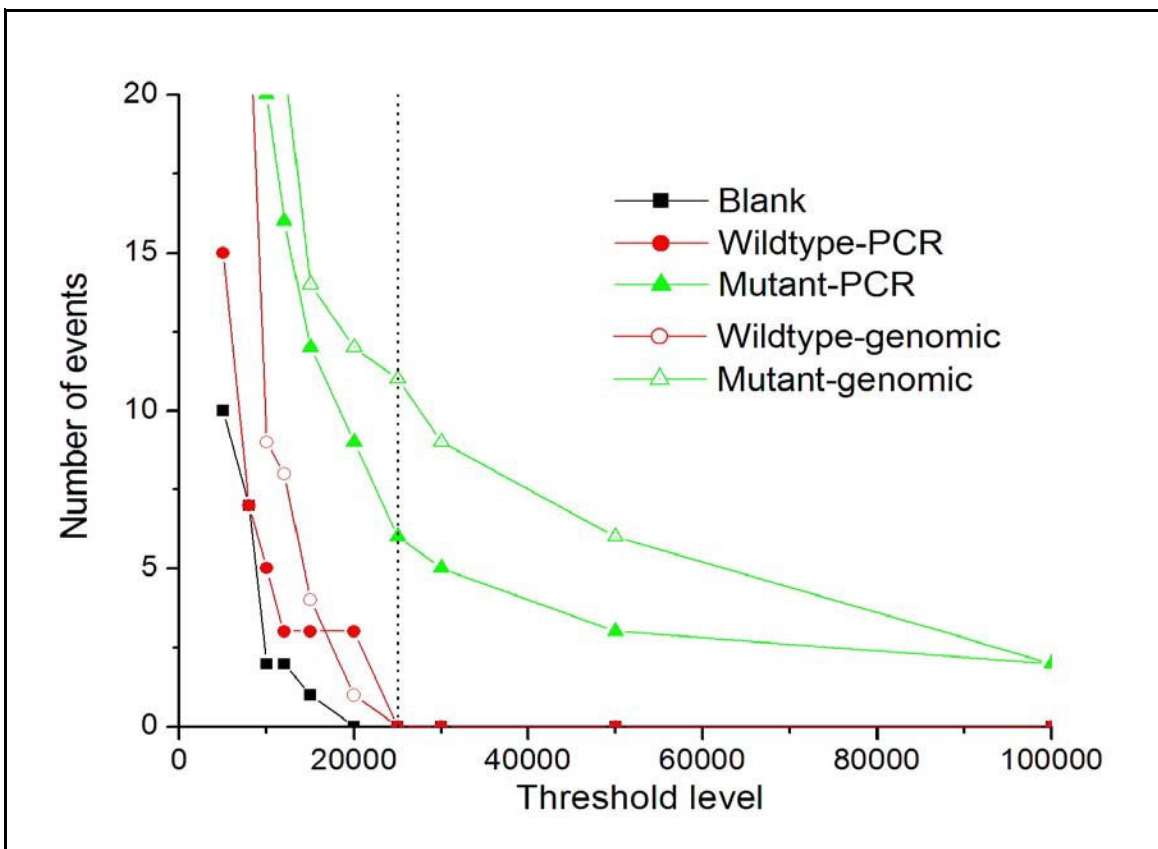


Figure 4. Plots showing number of events counted versus threshold level of a 20 cycle LDR reaction having $\sim 3,000$ copies of initial template, 10 pM primer concentration. The templates used were diluted from PCR products genomic samples extracted from cell line of known k-ras gene. The dotted line indicates the threshold level, $S(t) = 25,000$ chosen to minimize the total probability error to zero.

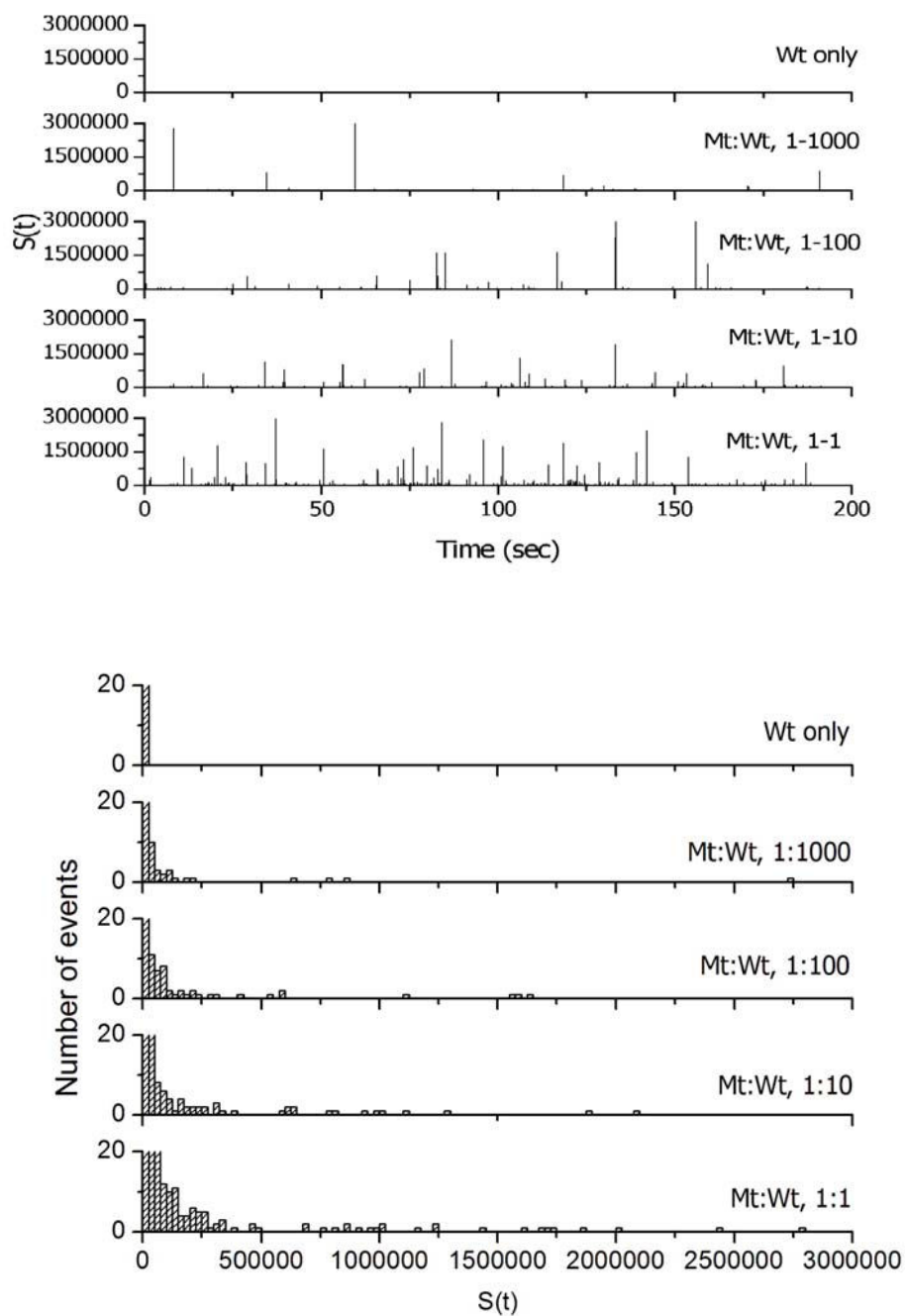
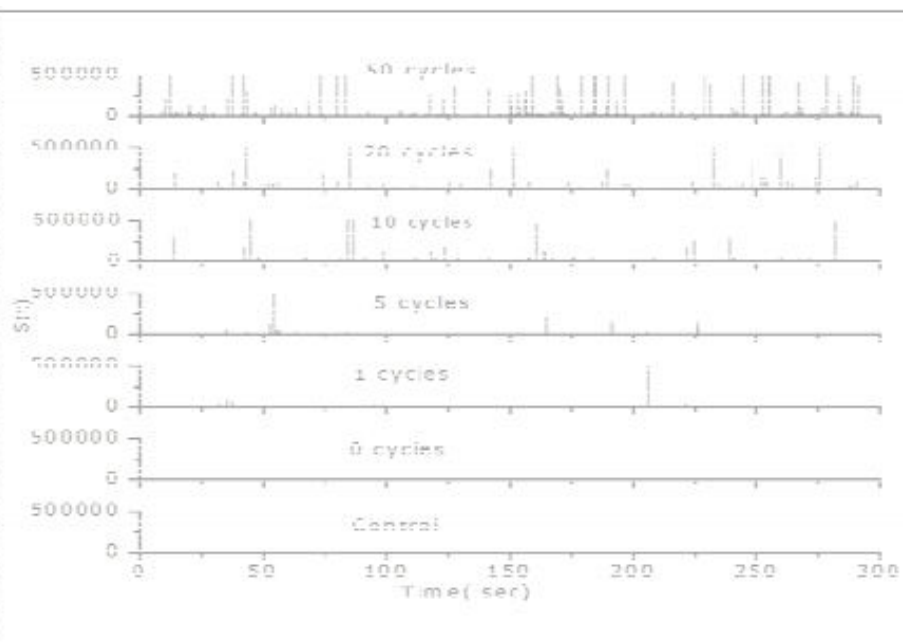


Figure 5. (A) Fluorescence bursts from individual LDR product undergoing spFRET and (B) histograms showing their distributions. Genomic samples with ratios of mt:wt ranging from 1:1 to 1: 1000 were used. The initial concentration of the mutant template in each assay was 2 ng. WQS filtered photon burst distributions were constructed using bin width of $S(t)$ = 25,000 counts.

A



B

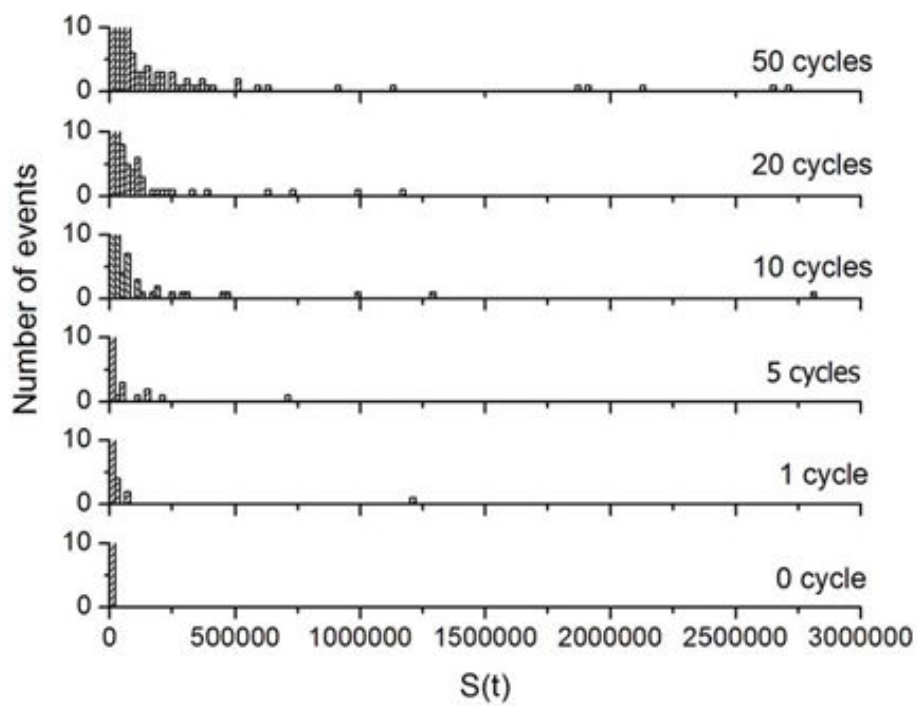
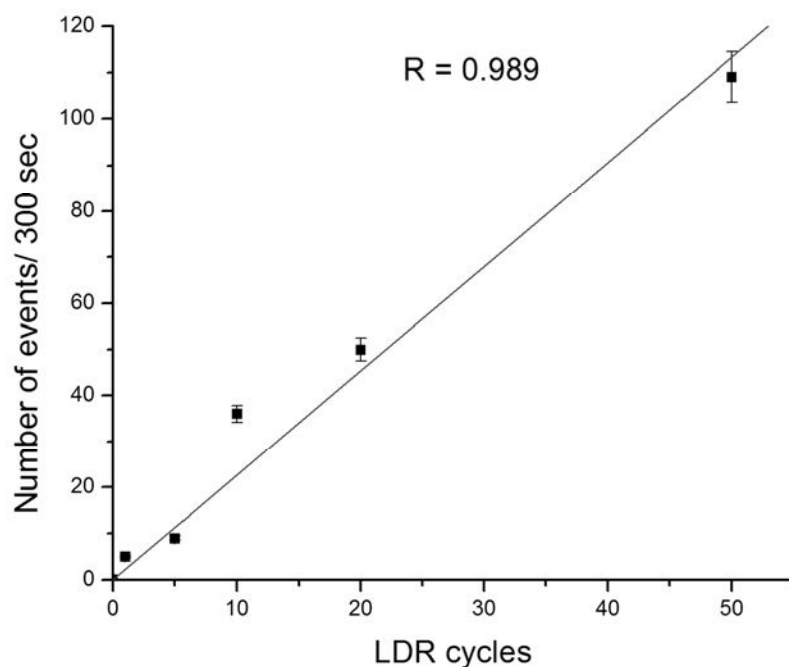


Figure 6 Plot showing the number of events detected from LDR hairpins in an LDR assay of matched ligation in the presence of excess mismatched template shown in Figure 7.



B

Figure 7 (A) Fluorescent bursts from individual LDR product undergoing various LDR thermal cycles. Genomic samples with a 1:10 ratio of mt:wt were used in the assay. Initial concentration of the mutant template in each assay was 2ng. (B) Linear calibration plot showing the number of LDR cycles versus number of fluorescence events from LDR product undergoing spFRET. Data was acquired over 300 s.

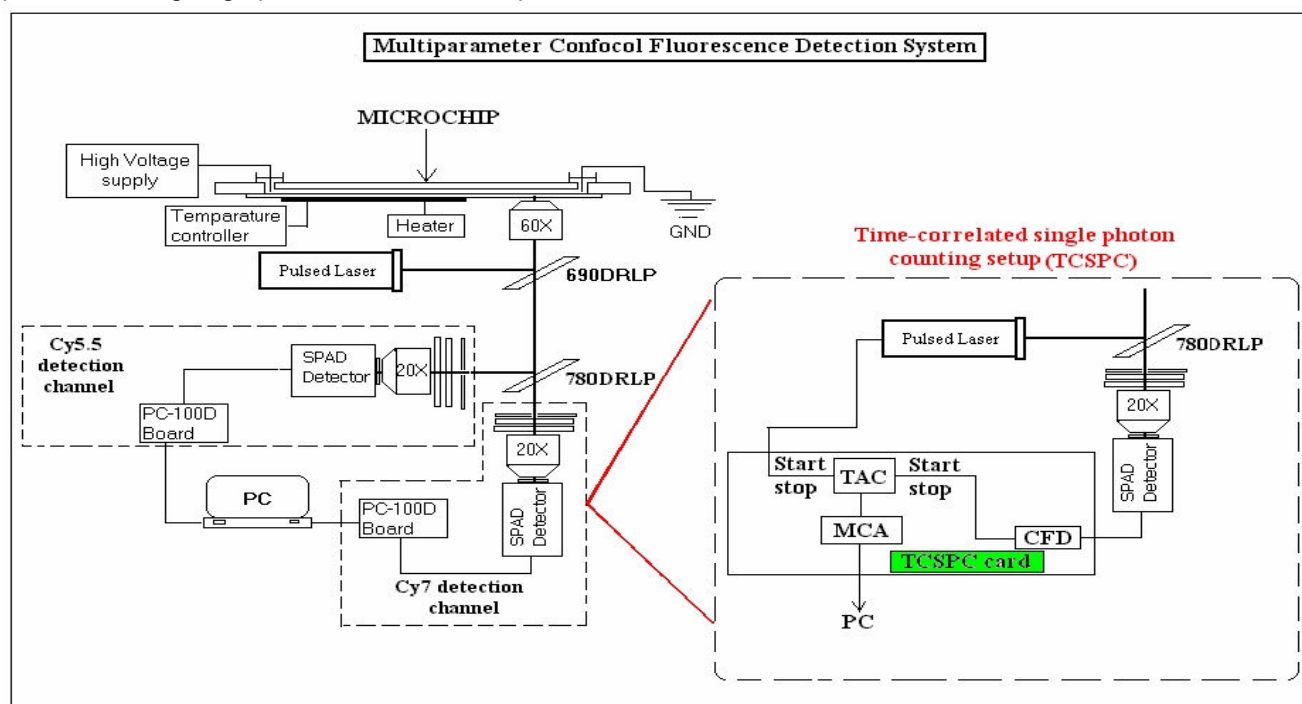


Figure 8 A schematic of a multiparameter confocal detection system used for SMD in microfluidic devices. The dualcolor unit consists of a diode laser (λ -635 nm) that is directed into a 60X objective using the first dichroic (D_1) mirror and focused into the microfluidic channel. The fluorescence collected by same objective is the transmitted through D_1 and D_2 where the transmitted light is imaged onto a pinhole and processed using a single photon avalanche diode (SPAD) in the first channel(780 channel). On the other hand, the reflected emission at D_2 dichroic is imaged onto a pinhole and processed using a second SPAD in the second channel (700 channel). TCSPC setup would consist of a pulsed laser and TCSPC card in each channel (see diagram).

